A full-scale static radar cross-section (RCS) measurement facility

J.W. Odendaal[a*], L. Botha[b] and J. Joubert[a]

We present an overview of a full-scale static RCS near-field measurement facility, and some sample measurements. The measurements, and the target, are in the near-field RCS range. Corrections for distance are made using sophisticated software.

To measure a structure's far-field radar scattering signature, it should be illuminated with a local plane wave; that is, the illuminating phase front must be planar. Several types of ranges are in use today to characterize the scattering properties of bodies. The most straightforward is the free-space range, in which the physical separation between the illuminating antenna and the target is relied upon to create the local plane wave in the test zone.[1] Large separation distances are required to measure sizeable objects. Near-field radar cross-section (RCS) measurements are a much more complex alternative because the target's scattering pattern depends on the physical nature of the object and on the electromagnetic field that illuminates it. Various techniques for near-field RCS measurements are reviewed in ref. 2. Falconer[3] proposes an extrapolation technique to determine the far-field RCS of targets using surface currents obtained from near-field measurements. Melin[4] applied a low pass filter to near-field data to obtain an approximation for the far-field RCS. Lamb[5] presented data for a flat plate measured in the near field. Time domain data (down-range profiles) are used in refs 6 and 7 to predict far-field RCS using data measured in the near field. Far-field data are presented for a target measured on a conducting ground plane in an anechoic chamber in ref. 8.

In this article, we discuss the implementation of a near-field measurement facility for static RCS measurements, give an overview of a full-scale facility and present some preliminary measurements. Approximate far-field RCS values are obtained using a near field to far field transformation based on radar imaging theory.[9,10] The technique was demonstrated in ref. 9 using near-field data measured in an anechoic chamber. The static near-field measurement facility can be used for ground-based diagnostic applications on large full-scale radar targets, such as aircraft and armoured vehicles. The facility is suitable for quality control measurements to identify and locate defects in backscattering properties of targets using radar images, from which areas of non-conformance relative to a benchmark object can be identified. The facility is also suitable for RCS signature management and to evaluate the effect of RCS modifications on targets. These comparisons can be evaluated quantitatively because the total far-field RCS of the various targets is estimated. Our ultimate aim is to establish a full-scale measurement facility suitable for RCS acceptance tests to be performed on airframes as well as ground-based vehicles.

Layout and measurement procedure

The layout of the full-scale RCS measurement facility is shown in Fig. 1 and consists of a pedestal, 8 m in diameter, a tower housing the transmit/receive antenna, an absorber between the antenna tower and target area to reduce ground bounce as well as target–ground interactions, and a climate-controlled laboratory housing the radar system and computer controllers.

The equipment is designed for RCS measurements of targets up to 18 m in length and/or width (such as typical airframe structures, with a much smaller height dimension as seen from the antenna) at frequencies between 300 MHz and 18 GHz. This wide frequency range is covered in three bands, namely, 300 MHz–2 GHz, 2–6 GHz and 6–18 GHz. To correct for the near-field scattering measurements using radar imaging techniques, the data are collected as a function of frequency and aspect angle. Typical measurements are performed over a stepped CW bandwidth of 2 GHz with a frequency resolution of 2.5 MHz, corresponding to 801 frequency samples. To increase measurement sensitivity, pulsed CW measurements are performed using hardware gating. The distance between the target's centre of rotation and antenna is adjustable between 20 m and 26.5 m. The height of the antenna above ground is adjustable from 0 to 10 m. The pedestal can support targets with a maximum mass of 18 tonnes. The read-back positional accuracy of the pedestal is 0.005° and the minimum speed of rotation is 0.001°/s. The time required to measure an 18-m target over a 90° angular sector is typically 3 h.

The measurement procedure consists of the following tasks: place absorber between the radar and target and underneath the target; perform a loop-back test on the radar to ensure proper operation; set timing parameters for the frequency band of interest, corresponding to the size of the target; set pedestal rotation speed parameters to comply with the required angular increments for radar imaging. (At this stage, the measurement parameters such as frequency span, frequency step size, number of averages, and angular step size must be fixed.); generate preliminary images to ensure appropriate parameters have been selected; perform measurements on the target. (Each measurement

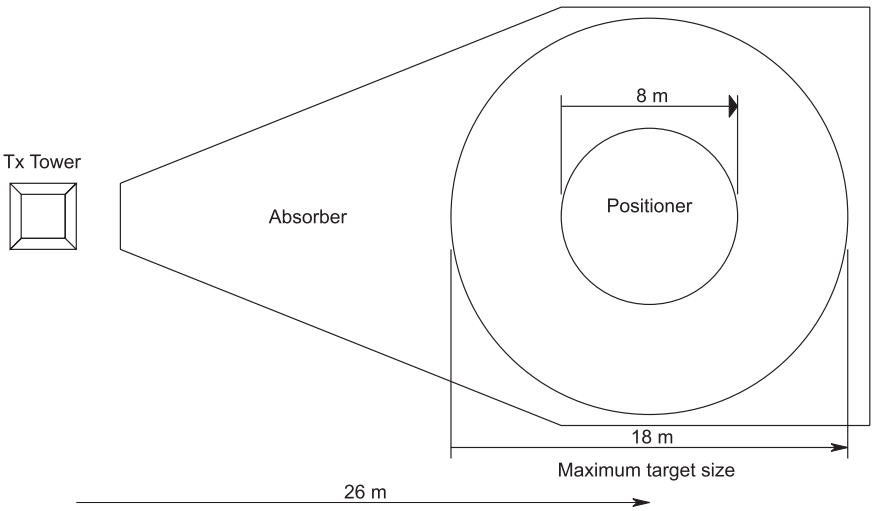

Fig. 1. Layout of the RCS measurement facility.

[a]Centre for Electromagnetism, Department of Electrical, Electronic and Computer Engineering, University of Pretoria, Pretoria 0002, South Africa.
[b]CSIR, P.O. Box 395, Pretoria 0001.
*Author for correspondence.
E-mail: wimpie.odendaal@up.ac.za

consists of frequency sweeps while the target is slowly rotated.); determine the calibration factor using at least one measurement on an empty platform (to estimate the noise level for the measurements) and one measurement using a known calibration target (usually a corner reflector or sphere); generate ISAR images and calculate RCS values for the target.

Sample measurements

The facility's performance is demonstrated using several targets—spheres of varying diameter and trihedral corner reflectors are measured individually and the resulting measured far-field RCS is compared with theory.

The results recorded for spheres of different sizes and a trihedral corner reflector, measured individually and calibrated using a 750-mm sphere as reference target, is shown in Fig. A in online supplementary material for a frequency of 9.5 GHz. The diameters of the spheres vary between 153 mm and 750 mm, relating to RCS values between –20 dBsm and 0 dBsm.

The test target, consisting of various generic scatterers on the pedestal, is shown in Fig. 2. The various spheres with two trihedral corner reflectors at the back and a long circular cylinder are clearly identifiable in the picture. Figure 3 shows an ISAR image of the test target generated using the data measured in the near field. The contributions from the two spheres in the front are evident in the image. The other two spheres are almost completely obscured by the PVC cylinders supporting the first sphere, and the first sphere itself, respectively. The contributions from the two trihedral corner reflectors are noticeably obscured by the objects closer to the radar source. Figure B in online supplementary material compares measured and simulated RCS values for the test target at 9.5 GHz.

As a further example, Fig. C online shows a Mirage F1 airframe as target on the measurement platform with the antenna tower and climate-controlled laboratory in the background. The area below the airframe and between target and antenna tower is covered with radar absorbing material to reduce the ground bounce contribution and interactions between the target and the ground. The resulting radar image of the F1 illuminated almost nose on is shown in Fig. 4. The scattering contributions from the nose, engine inlets and wing profiles can clearly be seen in the image, from which it is also evident that considerable energy is propagating into the engine inlet cavities

Fig. 2. Test target on the measurement platform.

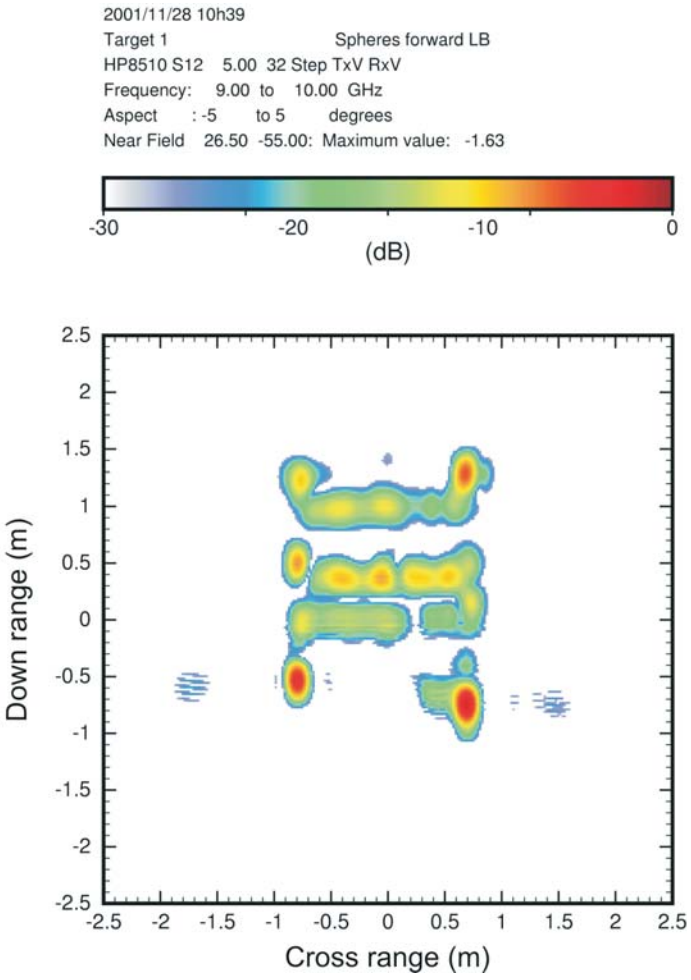

Fig. 3. ISAR image of the test target.

down to the engine and compressor plates and is scattered back to the receiving antenna and radar system.

Conclusion

Our facility allows full-scale RCS measurements from 300 MHz to 18 GHz of targets up to 18 m in size and weighing 30 tonnes. Good quality radar images are obtained that are useful for signature management and diagnostic purposes. Absolute far-field RCS values were obtained for point targets down to RCS values of –20 dBsm. Reasonable far-field RCS results were also obtained for targets consisting of various generic scatterers. The ability to estimate absolute far-field RCS values for complex radar targets requires more validation and is being pursued.

One major limitation of this equipment for obtaining absolute far-field RCS values is the assumption that the target being considered is a typical airframe with much larger dimensions in the azimuth plane than in the elevation

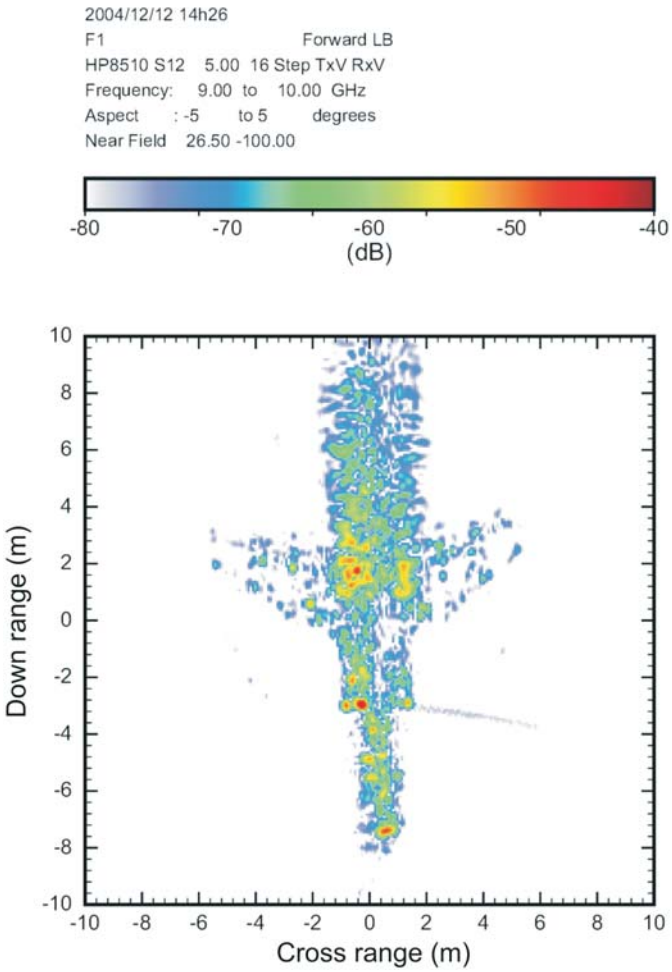

Fig. 4. ISAR image of the Mirage F1 airframe as seen from the front.

plane. Under this assumption, the resulting 2-D radar image is a good approximation to a similar image obtained from far-field RCS data. The approximation in the elevation plane can be improved with a significant increase in data collection and processing to generate 3-D radar images that also compensates for the finite distance to the scattering centres in the elevation plane.

This facility was developed under Armscor contract KT 434829 and is supported under Armscor contract KT 521861.

1. Currie N.C. (1989). *Radar Reflectivity Measurements: Techniques and Applications.* Artech House Inc., Norwood, MA.
2. Cown B.J. and Ryan C.E. (1989). Near-field scattering measurements for determining complex target RCS. *IEEE Trans. Antennas Propagat.* **37**, 576–585.
3. Falconer D.G. (1988). Extrapolation of near-field RCS measurements to the far zone. *IEEE Trans. Antennas Propagat.* **36**, 822–829.
4. Melin J.O. (1987). Measuring radar cross section at short distance. *IEEE Trans. Antennas Propagat.* **35**, 991–996.
5. Lamb B.M. (1991). Approximation of far-field illumination conditions through transformation of near-field RCS data. *Proc. 1991 National Radar Conference,* pp. 152–155, Los Angeles, CA.
6. Chang D.C., Tzay M.C. and Chung R.C. (2001). Far field RCS prediction by near field RCS measurements. *Proc. Asia Pacific Microwave Conference,* pp. 1239–1242, Taipei.
7. Chang D.C. and Tsai M.C. (2002). Far field RCS prediction by near field RCS measurements. *IEEE Antennas and Propagation Society International Symposium,* pp. 106–109, San Antonio, Texas.
8. Inasawa Y., Kuroda S. and Morita S. (2005). Far-field RCS prediction from measured near-field data including metal ground bounce. *IEEE/ACES International Conference on Wireless Communications and Applied Electromagnetics,* pp. 913–916, Honolulu, Hawaii.
9. Odendaal J.W. and Joubert J. (1996). Radar cross section measurements using near-field radar imaging. *IEEE Trans. Instrumentation Measurement* **45**, 948–954.
10. Broquetas A., Palau J., Jofre L. and Cardama A. (1998). Spherical wave near-field imaging and radar cross-section measurements, *IEEE Trans. Antennas Propagat.* **46**, 730–734.

This article is accompanied by supplementary material online at www.sajs.co.za

Supplementary material to:

Odendaal J.W., Botha L. and Joubert J. (2007). A full-scale static radar cross-section (RCS) measurement facility. *S. Afr. J. Sci.* **103**, 196–198.

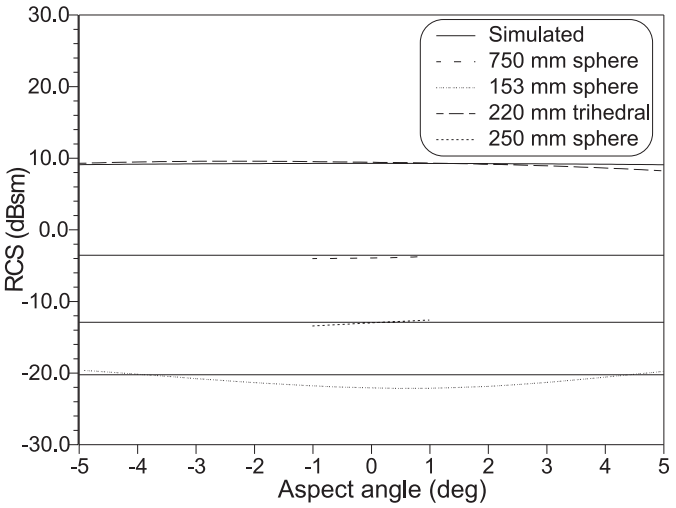

Fig. A. Measured results of individual generic targets.

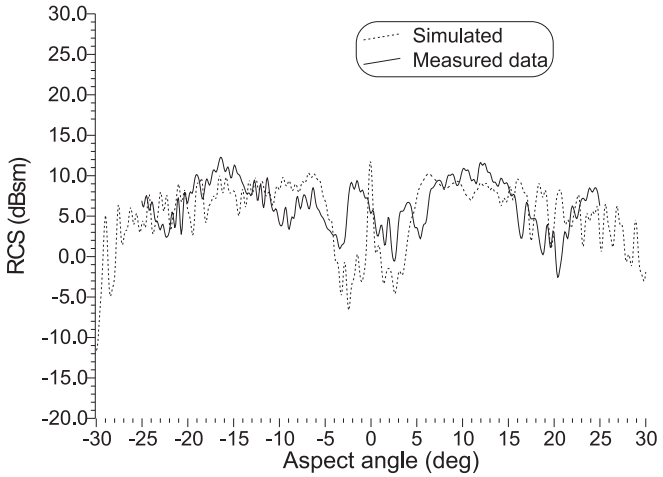

Fig. B. Comparison of theoretical values and far-field RCS data for the test target.

Fig. C. The Mirage F1 airframe on the measurement platform. The antenna tower and laboratory can be seen in the background.